PAPER

NJC
www.rsc.org/njc

Effect of carboxylate spacers on the supramolecular self-assembly of dicopper(II) Schiff base complexes stabilizing water assemblies of different conformations† ‡

Arindam Mukherjee, Manas K. Saha, Munirathinam Nethaji and Akhil R. Chakravarty*

Department of Inorganic and Physical Chemistry, Indian Institute of Science, Bangalore, 560012, India. E-mail: arc@ipc.iisc.ernet.in; Fax: +91-80-23600683

Received (in Montpellier, France) 14th October 2004, Accepted 5th January 2005
First published as an Advance Article on the web 3rd March 2005

Dicopper(II) complexes, namely $[Cu_2L(O_2C\text{–}CH{=}CH\text{–}C_6H_4\text{-}p\text{-}OH)]\cdot 2H_2O$ (**1**·2H_2O), $[Cu_2L(O_2C\text{–}CH_2\text{–}C_6H_4\text{-}p\text{-}OH)]\cdot 2H_2O$ (**2**·2H_2O) and $[Cu_2L(O_2C\text{–}CH_2CH_2\text{–}C_6H_4\text{-}p\text{-}OH)]\cdot 0.5H_2O$ (**3**·0.5H_2O), having different carboxylate ligands with a *p*-hydroxyphenyl moiety and the pentadentate Schiff base *N*,*N*′-1,3-diylbis(salicylaldimino)propan-2-ol (H_3L) in its trianionic form, were prepared and structurally characterized by X-ray crystallography. The complexes have a dicopper(II) unit with an alkoxo bridge from the Schiff base and the carboxylate, showing a three-atom bridging mode. The metal centres in a square planar $CuNO_3$ coordination geometry are antiferromagnetically coupled in the asymmetrically double-bridged dicopper(II) core. A significant effect of the –CH=CH–, $–CH_2–$ and $–CH_2CH_2–$ spacers of the carboxylate ligands on the formation of different supramolecular structures is observed. Complex $[Cu_2L(O_2C\text{–}CH{=}CH\text{–}C_6H_4\text{-}p\text{-}OH)]$, **1**, forms a helical supramolecular structure due to hydrogen-bonding interactions involving the *p*-hydroxy group of the phenol from the carboxylate and one phenoxo oxygen atom from the Schiff base. The lattice waters form a helical one-dimensional chain, in which alternate water molecules are anchored to the supramolecular host and the chain propagates along the crystallographic 2_1 screw axis. Complex **2** forms water aggregates of quasi-linear and pseudo-hexameric cyclic chair conformations involving lattice water molecules, and the previously mentioned para OH group phenoxo oxygen atom. Complex **3**·0.5H_2O shows the formation of a supramolecular one-dimensional chain structure due to hydrogen-bonding interactions between the *p*-OH group and the phenoxo oxygen atom. Two such supramolecular structures are linked by hydrogen-bonding interactions involving the lattice water. Differential scanning calorimetry (DSC) of **1**·2H_2O gives two endotherms at 61.5 and 88.5 °C for the loss of the "free" and the "anchored" water molecules, respectively. The overall change of enthalpy per water molecule is ~ 36 kJ mol^{-1}. Complex **2**·2H_2O shows an endotherm at 131 °C with a shoulder at ~ 126 °C. The enthalpy change per water molecule is ~ 26 kJ mol^{-1}. The reversibility in loss or addition of lattice water molecules and the corresponding effect on the overall structure is probed by X-ray powder diffraction studies.

Introduction

The structural and dynamical aspects of water molecules in confined or constricted spaces, such as in the cavities or channels of supramolecular structures that are largely prevalent in biological systems and in inorganic solids, are of considerable current importance to understand the behaviour of such water molecules in a variety of hydrophilic and/or hydrophobic environments.[1–5] The properties of water molecules in the aggregate form showing different morphologies often vary significantly from those of bulk water in the solid (*i.e.*, ice) or liquid phases. While water molecules are ubiquitous as the solvent of crystallization in crystal lattices, observation of water aggregates having structures similar to those found in bulk water or in biological systems are limited[6–18] and such water assemblies could be used as potential models to gain a better insight into the nature of hydrogen bonding, its morphology and the dynamical aspects of these water molecules. Among the different morphologies that water aggregates of composition $(H_2O)_n$ ($n > 2$) can assume, the cyclic and cage structures are rather common and are known to be more stable than a linear chain structure.[1,4] While the cage structures of water molecules in crystal hosts provide models for bulk water, single file linear chain structures of water aggregates are likely to model systems such as the biological membrane water channel in aquaporin-1 or the ion channel of gramicidin A.[19–22]

Water molecules play an important role in the formation of supramolecular structures involving hydrogen bonds of varied strengths and become an integral part of such self-assembled structures.[12,23] Alternatively, a supramolecular host could lead to the formation of unusual water aggregates that are more dynamic in nature, such as found in biological systems. The present work stems from our interest to synthesize alkoxo-carboxylato double-bridged dicopper(II) complexes as host structures using carboxylate ligands with pendant hydroxyl groups that could participate in hydrogen-bonding interactions between the ligand and lattice solvent molecule(s) to form new supramolecular structures. We have shown in a preliminary communication that the Schiff base dicopper(II) complex $[Cu_2L(O_2C\text{–}CH{=}CH\text{–}C_6H_4\text{-}p\text{-}OH)]\cdot 2H_2O$ (**1**·2H_2O), where L is the trianionic form of *N*,*N*′-1,3-diylbis(salicylaldimino)propan-2-ol (H_3L), forms an unprecedented type of one-dimensional helical chains of hydrogen-bonded water molecules, anchored onto a helical supramolecular host resulting from

---

† Dedicated to Prof. Animesh Chakravorty on his 70th birthday.

‡ Electronic supplementary information (ESI) available: variable temperature magnetic susceptibility data for the complexes (Tables S1–S3), ORTEP diagrams of the complexes **1**·2H_2O and **3**·0.5H_2O (Figs. S1, S2). See http://www.rsc.org/suppdata/nj/b4/b415945d/

DOI: 10.1039/b415945d

the self-assembly of the dicopper(II) complex.[24] It was determined that the dihedral angle between the –CH=CH–C_6H_4– (styrene) unit of the *p*-hydroxycinnamate ligand and the basal coordination plane of $\{Cu_2L\}^+$ was a crucial parameter in the formation of a helical structure. We have since investigated in detail the role of the spacer in the carboxylate ligand on the supramolecular structure by using two additional carboxylates, from *p*-hydroxyphenylacetic acid (–CH_2–) and *p*-hydroxyphenylpropionic acid (–CH_2CH_2–, Scheme 1). The corresponding complexes $[Cu_2L(O_2C–CH_2–C_6H_4\text{-}p\text{-}OH)]\cdot 2H_2O$ (**2**·$2H_2O$) and $[Cu_2L(O_2C–CH_2CH_2–C_6H_4\text{-}p\text{-}OH)]\cdot 0.5H_2O$ (**3**·$0.5H_2O$) have been prepared and their crystal structures determined. Herein, we present the supramolecular chemistry of these three complexes, showing the significant geometrical control exerted by the carboxylate spacers on the formation of water aggregates. The ability of the complexes to reversibly dehydrate is investigated by powder X-ray diffraction methods.

Experimental

Materials and instruments

All chemicals were purchased from commercial sources and used as received. The Schiff base *N*,*N*′-1,3-diylbis(salicylaldimino)propan-2-ol (H_3L) and the dicopper(II) precursor complex $[Cu_2L(O_2CCH_3)]$ were prepared by a literature method.[25] Elemental analyses were done using a Thermo Finnigan FLASH EA 1112 CHNS analyzer. UV-Vis and infrared spectra were recorded from Hitachi U-3400 and Bruker Equinox 55 spectrometers, respectively. X-Ray powder diffraction data were recorded on a Philips X'Pert diffractometer. TGA analyses were performed on a Mettler Toledo Star thermal analyzer. Differential scan calorimetric (DSC) data were obtained from a Rheometric Scientific DSC Plus instrument.

Magnetic measurements

Variable temperature magnetic susceptibility data for the polycrystalline samples were obtained in the temperature range 18–300 K using a model 300 Lewis coil force magnetometer from George Associates, Inc. (Berkeley, USA) equipped with a Cahn balance and a closed-cycle cryostat (Air Products). $Hg[Co(NCS)_4]$ was used as a standard. Experimental susceptibility data were corrected for diamagnetic contributions and for the temperature-independent paramagnetism ($N_\alpha = 60 \times 10^{-6}$ cm^3 mol^{-1} per copper). The molar magnetic susceptibilities were fitted by the modified Bleaney–Bowers expression by means of a least-squares computer program.[26,27] The Hamiltonian and susceptibility equation used were: $\hat{H} = -2J(\hat{S}_1\hat{S}_2)$, where $S_1 = S_2 = 1/2$ for a d^9-d^9 dicopper(II) core, and $\chi_{Cu} = [Ng^2\beta^2/k(T-\theta)][3+\exp(-2J/k(T-\theta)]^{-1}(1-\rho)+(Ng_1{}^2\beta^2/4kT)\rho + N_\alpha$, where ρ is the fraction of monomeric impurity and $2J$ is the singlet–triplet separation energy. The magnetic moments were calculated in μ_B unit.

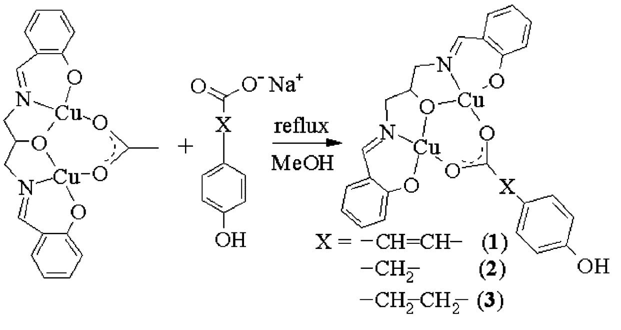

Scheme 1 Synthetic scheme for the preparation of asymmetrically double-bridged dicopper(II) complexes **1–3**, with different X spacers in the carboxylate ligand.

Syntheses

$[Cu_2L(O_2C–CH=CH–C_6H_4\text{-}p\text{-}OH)]$ (1). $[Cu_2L(O_2CCH_3)]$ (0.65 g, 1.35 mmol) in MeOH (50 ml) was reacted with the sodium salt of *p*-hydroxycinnamic acid (0.25 g, 1.35 mmol) under refluxing conditions for 30 min. The solution was cooled to ambient temperature and filtered. The product was isolated in good yield (0.5 g, ~65%) as a green solid by slow concentration of the filtrate. Anal. calcd for $C_{26}H_{22}Cu_2N_2O_6$ (M 585.54): C 53.33, H 3.79, N 4.78%; found: C 53.04, H 3.92, N 5.06%; UV-Vis in THF [λ_{max}/nm (ε/dm^3 mol^{-1} cm^{-1})]: 639 (350), 377 (9100), 277 (31 000), 247 (33 500), 227 (47 600); IR (KBr, cm^{-1}; br, broad; w, weak; m, medium; s, strong): 3368 br, 3059 w, 3020 w, 2931 w, 2904 w, 1635 s, 1617 m, 1534 s, 1508 s, 1451 s, 1397 s, 1296 m, 1243 m, 1198 m, 1159 m, 1129 w, 987 w, 897 w, 840 m, 760 m, 703 m, 566 w, 456 w, 429 w; μ_{eff} (per copper)/μ_B: 1.67 at 300 K; 0.36 at 18 K; $2J = -116$ cm^{-1} from theoretical fitting with $g = 2.01$, $\rho = 0.015$, $g_1 = 2.2$, $\theta = 1.5$ K, $R = 7.2 \times 10^{-3}$ (where $R = \sum_i[[\chi_{obs}(T_i) - \chi_{calcd}(T_i)]^2/\chi_{obs}(T_i)^2]$).

$[Cu_2L(O_2CCH_2C_6H_4\text{-}p\text{-}OH)]$ (2). $[Cu_2L(O_2CCH_3)]$ (0.65 g, 1.35 mmol) in MeOH (20 ml) was reacted with the sodium salt of *p*-hydroxyphenylacetic acid, prepared *in situ* from the acid (0.21 g, 1.35 mmol) and NaOH (0.05 g, 1.3 mmol) in ethanol (5 ml). The mixture was refluxed for 30 min, followed by cooling to 25 °C, and was then filtered. The filtrate was slowly concentrated to give **2** as a green solid (0.55 g, yield: ~70%). Anal. calcd for $C_{25}H_{22}Cu_2N_2O_6$ (M 573.53): C 52.35, H 3.87, N 4.88%; found: C 52.58, H 4.03, N 4.76%; UV-Vis in THF [λ_{max}/nm (ε/dm^3 mol^{-1} cm^{-1})]: 640 (330), 376 (9200), 272 (29 100), 242 (40 000); IR (KBr, cm^{-1}): 3387 br, 2931 w, 1634 s, 1602 m, 1573 s, 1539 m, 1516 m, 1470 m, 1450 s, 1404 s, 1343 m, 1304 m, 1249 w, 1198 m, 1154 m, 1131 m, 1032 w, 975 w, 897 w, 859 w, 794 w, 762 s, 742 w, 702 m, 650 w, 600 m, 555 m, 466 w; μ_{eff} (per copper)/μ_B: 1.59 at 300 K; 0.19 at 18 K; $2J = -176$ cm^{-1} from theoretical fitting with $g = 2.06$, $\rho = 0.009$, $g_1 = 2.15$, $\theta = 2$ K, $R = 7.7 \times 10^{-3}$.

$[Cu_2L(O_2CCH_2CH_2C_6H_4\text{-}p\text{-}OH)]$ (3). **3** was prepared by a procedure similar to that of complex **2** with *p*-hydroxyphenylpropionic acid instead of *p*-hydroxyphenylacetic acid. Yield: ~61%; anal. calcd for $C_{26}H_{24}Cu_2N_2O_6$ (M 587.55): C 53.15, H 4.12, N 4.76%; found: C 53.07, H 4.20, N 4.89%; UV-Vis in THF [λ_{max}/nm (ε/dm^3 mol^{-1} cm^{-1})]: 640 (370), 376 (9300), 272 (30 000), 247 (41 500); IR (KBr, cm^{-1}): 3350 br, 3021 br, 2908 m, 1637 s, 1601 m, 1513 s, 1472 m, 1447 s, 1397 m, 1342 m, 1314 s, 1197 s, 1156 m, 1130 m, 1103 w, 1056 w, 971 w, 909 w, 895 w, 855 w, 874 w, 829 m, 794 m, 756 s, 740 m, 703 s, 607 m, 572 m, 490 w, 464 w; μ_{eff} (per copper)/μ_B: 1.75 at 300 K; 0.22 at 18 K; $2J = -140$ cm^{-1} from theoretical fitting with $g = 2.18$, $\rho = 0.013$, $g_1 = 2.2$, $R = 5.9 \times 10^{-3}$.

X-Ray crystallography

Single crystals of the complexes were obtained from slow concentration of the complex solutions in aqueous methanol. A green crystal of **1**·$2H_2O$ of size 0.2 × 0.1 × 0.05 mm^3 was mounted on a glass fibre with epoxy cement and all geometric and intensity data were collected using an automated Enraf–Nonius CAD4 diffractometer fitted with MoKα radiation. Intensity data, collected using the ω scan technique for 2545 reflections in the range $1.62° \le \theta \le 24.99°$, were corrected for Lorentz polarization effects and for absorption.[28] Of 2545 unique data, 1799 with $I \ge 2\sigma(I)$ were used for structure determination involving 363 parameters, giving a goodness-of-fit value of 0.977 and highest shift/e.s.d. value of 0.003. All nonhydrogen atoms were refined anisotropically. The hydrogen atoms attached to the oxygen atoms were located from the difference Fourier map and refined isotropically using geometrical restraints, while those attached to the carbon atoms were generated and refined using a riding model with fixed thermal parameters.

Geometric and intensity data for **2**·$2H_2O$ (crystal size: $0.36 \times 0.08 \times 0.02$ mm^3) and **3**·$0.5H_2O$ (crystal size: $0.28 \times 0.19 \times 0.02$ mm^3) were collected using a Bruker SMART APEX CCD diffractometer having a fine focus and a 1.75 kW sealed tube MoKα X-ray source with increasing ω (width of 0.3° frame^{-1}) at a scan speed of 12 s frame^{-1}. The data were corrected for absorption.[29] A total of 8510 reflections were collected for **2**·$2H_2O$ in the range $1.26° \leq \theta \leq 24.71°$ of which 5567 reflections with $I \geq 2\sigma(I)$ were used for structure solution using 689 parameters, giving a goodness-of-fit value of 1.143 and highest shift/e.s.d. value of 0.001. All nonhydrogen atoms, except for two positionally disordered oxygen atoms, were refined anisotropically for **2**·$2H_2O$. The oxygen atoms of two lattice water molecules showed positional disorder and two sets of atoms, namely O(15), O(16) and O(15A), O(16A), were refined with site occupancies of 0.7 and 0.3, respectively. The hydrogen atoms attached to the carbon atoms were fixed in their calculated positions and refined using a riding model. The hydrogen atoms of the *p*-hydroxy groups and the non-disordered water molecules were located from the difference Fourier map and refined with an O–H bond distance constraint of 0.96 Å. There were two dimeric complexes and four water molecules (in total) in the crystallographic asymmetric unit of **2**·$2H_2O$ in the triclinic space group $P\bar{1}$, possibly due to the presence of two different water aggregates in the structure. For **3**·$0.5H_2O$, a total of 4128 reflections were collected in the range $1.74 \leq \theta \leq 24.71$ of which 3534 reflections with $I \geq 2\sigma(I)$ were used for structure solution using 409 parameters giving a goodness-of-fit value of 1.075 and highest shift/e.s.d. value of 0.002. All nonhydrogen atoms were refined anisotropically, except for O(7), which was modelled as a disordered lattice water molecule with a site occupancy of 0.5. Hydrogen atoms attached to carbon atoms were generated and refined using a riding model.

The structure solution and refinement were made using SHELX programs.[30] Perspective views of the molecules were obtained by ORTEP.[31]

Results and discussion

Synthesis and general aspects

Dicopper(II) complexes **1–3** were prepared in good yields from a general reaction involving substitution of the bridging acetate in $[Cu_2L(O_2CCH_3)]$ by the carboxylate ligand HO-*p*-C_6H_4–X–CO_2^-, where X is the spacer (–CH=CH–, –CH_2– or –CH_2CH_2–, respectively; Scheme 1). The complexes crystallize with lattice water molecules. We have shown in a previous study that a similar reaction with *p*-hydroxybenzoate (HO–*p*-$C_6H_4CO_2^-$), which lacks the spacer X, leads to the formation of a discrete tetranuclear copper(II) complex $[Cu_4L_2(O_2C–C_6H_4$-*p*-$OH)_2]$ in which two $\{Cu_2L(O_2C–C_6H_4$-*p*-$OH)\}$ units are covalently linked through the phenoxo oxygen atom of the Schiff base ligand, showing axial/equatorial bonding modes.[32] This tetranuclear complex does not form any supramolecular structure: it crystallizes with one lattice isopropanol molecule (and not with water from the aqueous alcohol), which is involved in hydrogen-bonding interactions with the *p*-hydroxy group of the carboxylate, resulting in the discrete nature of the complex. However, with the inclusion of spacers, complexes **1–3** are dimeric in nature and form a variety of supramolecular structures, involving the lattice water molecules.

The complexes are soluble in polar organic solvents and display a d-d band at 640 nm in THF. Having an asymmetrically double-bridged dicopper(II) core with a *syn,syn*-bonded carboxylato and a monoatomic alkoxo bridges, they show antiferromagnetic properties with a singlet–triplet separation energy (2*J*) in the range from -116 to -176 cm^{-1} (with the singlet as the ground state; Fig. 1). The magnitude of *J* in such $\{Cu_2(\mu\text{-}OR)(\mu\text{-}O_2CR)\}$ cores is generally small due to the noncomplementary nature of the super-exchange pathways involving symmetric (φ_{sym}) and antisymmetric (φ_{asym}) combinations of magnetic orbitals.[24,33,34] The $2J$ values observed for **1–3** compare well to that of the precursor complex (-170 cm^{-1}).[25]

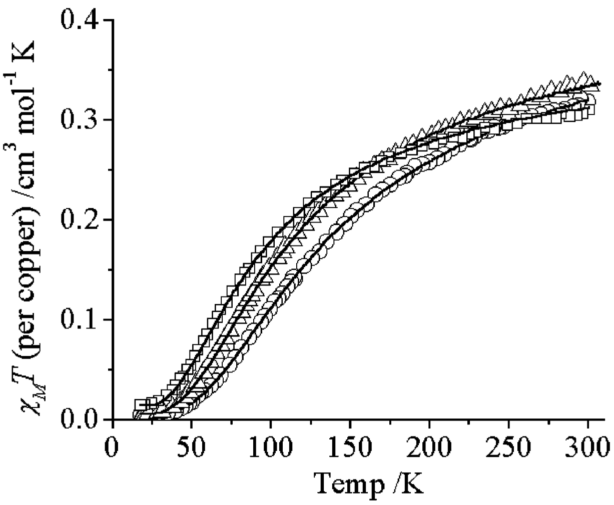

Fig. 1 $\chi_M T$ *vs.* *T* plots for complexes **1–3**; the solid lines show the theoretical fit to the experimental data (□: **1**; ○: **2**; △: **3**).

Crystal structures

All three complexes are structurally characterized by single crystal X-ray crystallography. Selected crystallographic data for **1–3** are given in Table 1.§ Relevant bond distances and angles are given in Tables 2 and 3. Selected hydrogen-bonding parameters are presented in Table 4. Complex **1**·$2H_2O$ crystallizes in the orthorhombic space group $P2_1nb$ with four dicopper(II) units in the unit cell. The complex self-assembles into a helical supramolecular structure through hydrogen-bonding interactions involving the pendant hydroxy group of the carboxylate and one phenoxo oxygen atom of the Schiff base L (Fig. 2). The cinnamate ligand forms an angle of ~30° with the plane of the $\{Cu_2L\}^+$ unit and such an inclination could be responsible for the formation of the helical structure. The supramolecular host forms a pore in which the lattice water molecules accumulate, forming an unprecedented helical one-dimensional chain, stabilized by anchoring to the host structure through hydrogen-bonding interactions involving alternating water molecules of the chain and the phenoxo oxygen atoms of the Schiff base. The hydrogen bonds, showing O···O distances of ~3.0 Å along the chain, are weak. Both water molecules are expected to be labile with the "free" water molecule being itself relatively more labile than the "host-bound" one. Although dynamic water molecules assuming a single file chain structure are known[19–22] in biological membrane proteins like aquaporin-1 and gramicidin A, an analogous one-dimensional chain in a crystal host is a rare occurrence. Buchanan and co-workers have reported one-dimensional water chains stabilized by imidazole channels in which all the water molecules are bonded to the organic host in a "zig-zag" motif.[8] Another report on self-assembled chains of tetrameric water aggregates in a crystal host comprised of 1,4,7,10-tetraazacyclodecane has been made recently by Samanta and co-workers.[9] While these water chains could have relevance to biological systems of water or ion transport, the

---

§ CCDC reference numbers: 222969 for **1**·$2H_2O$, 224514 for **2**·$2H_2O$ and 260832 for **3**·$0.5H_2O$. See http://www.rsc.org/suppdata/nj/b4/b415945d/ for crystallographic data in .cif or other electronic format.

Table 1 Crystallographic data for $[Cu_2L(O_2C–CH{=}CH–C_6H_4\text{-}p\text{-}OH)]\cdot 2H_2O$ (**1** · $2H_2O$), $[Cu_2L(O_2C–CH_2–C_6H_4\text{-}p\text{-}OH)]\cdot 2H_2O$ (**2** · $2H_2O$) and $[Cu_2L(O_2C–CH_2CH_2–C_6H_4\text{-}p\text{-}OH)]\cdot 0.5H_2O$ (**3** · $0.5H_2O$).

	1 · $2H_2O$	**2** · $2H_2O$	**3** · $0.5H_2O$
Formula	$C_{26}H_{26}Cu_2N_2O_8$	$C_{25}H_{26}Cu_2N_2O_8$	$C_{26}H_{25}Cu_2N_2O_{6.5}$
FW	621.57	609.56	596.56
Crystal system	Orthorhombic	Triclinic	Monoclinic
Space group	$P2_1nb$ (no. 33)	$P\bar{1}$ (no. 2)	$P2_1/c$ (no. 14)
a/Å	8.106(3)	10.861(2)	7.8190(10)
b/Å	13.166(3)	14.419(3)	22.534(5)
c/Å	25.160(4)	16.634(3)	13.699(2)
α/°	90	80.332(4)	90
β/°	90	80.068(4)	94.203(5)
γ/°	90	80.199(4)	90
U/Å^3	2685.2(12)	2502.5(8)	2407.2(7)
Z	4	4	4
ρ_{calcd}/g cm^{-3}	1.538	1.618	1.646
μ(MoKα)/cm^{-1}	16.35	17.52	18.15
T/K	293(2)	293(2)	293(2)
R_{int}	0.0	0.0985	0.0282
$R_1{}^a$	0.0546	0.0891	0.0370
R_1 (all data)	0.0931	0.1429	0.0463
$wR_2{}^b$	0.1399	0.1635	0.0906
wR_2 (all data)	0.1669	0.1842	0.0954

^{a} $R_1 = \sum||F_o| - |F_c||/\sum|F_o|$. ^{b} $wR_2 = \{\sum[w(F_o{}^2 - F_c{}^2)^2]/\sum[w(F_o{}^2)^2]\}^{1/2}$; $w = 1/[\sigma^2(F_o{}^2) + (AP)^2 + BP]$ where $P = [\max(F_o{}^2,0) + 2F_c{}^2]/3$ and A = 0.1108, 0.0595, 0.0609 and B = 0.0; 2.3093; 1.3998 for **1–3**, respectively.

helical water chain in a helical supramolecular host, as observed in **1** · $2H_2O$, is a good potential model, considering the helical nature of membrane proteins.

Complex **2** · $2H_2O$ crystallizes in the triclinic space group $P\bar{1}$ with two dicopper(II) complexes in the asymmetric unit (Z = 4). The dinuclear complex with a $\{Cu_2(\mu\text{-}OR)(\mu\text{-}O_2CR)\}$ core has a similar structure to that of **1**, where the monoatomic alkoxo bridge is derived from the pentadentate Schiff base and *p*-hydroxyphenylacetate is a three-atom bridging carboxylate (Fig. 3). Each copper has a planar $CuNO_3$ coordination geometry, giving a Cu···Cu distance and Cu–O(R)–Cu angle of ~3.5 Å and ~133°, respectively. What makes the structure of complex **2** significantly different from that of **1** is the angle of ~72° between the $–CH_2–C_6H_4\text{-}p\text{-}OH$ group and the $Cu_2N_2O_5$ plane. Such a stereochemical arrangement possibly prevents the phenoxo oxygen atoms in L from axial bonding to the copper centres. Complex **2** thus self-assembles into a different supramolecular structure, involving the pendant hydroxyl group of the carboxylate, the lattice water molecules and the phenoxo oxygen atom of the Schiff base. The lattice water molecules show two types of water aggregates: pseudo-hexameric cyclic chairs and quasi-linear forms. Unlike **1** · $2H_2O$, the supramolecular structure in **2** · $2H_2O$ includes the lattice water molecules as an integral part, thus making them relatively more stable in comparison to the helical water chain (Fig. 4). Fig. 5 shows the hydrogen-bonding network in the water aggregates in **2** · $2H_2O$. Water oxygen atoms O(13)#1, O(13)#2, O(14), O(14)#3 and hydroxy group atoms O(6), and O(6)#3 form together a cyclic hexameric structure, giving O···O distances in the range 2.74(9)–2.78(1) Å. In addition, the water molecules are also hydrogen-bonded to the phenoxo oxygen atoms of the Schiff base (O···O distance ~2.84 Å).

Table 2 Selected bond distances (Å) and angles (°) in **1** · $2H_2O$ and **3** · $0.5H_2O$

	1 · $2H_2O$	**3** · $0.5H_2O$
Cu(1)···Cu(2)	3.476(2)	3.464(2)
Cu(1)–O(1)	1.905(7)	1.879(2)
Cu(1)–O(2)	1.911(7)	1.904(2)
Cu(1)–O(5)	1.914(6)	1.932(2)
Cu(1)–N(1)	1.935(7)	1.925(3)
Cu(2)–O(2)	1.926(7)	1.894(2)
Cu(2)–O(3)	1.901(7)	1.894(2)
Cu(2)–O(4)	1.939(7)	1.904(2)
Cu(2)–N(2)	1.932(8)	1.902(3)
Cu(1)–O(2)–Cu(2)	129.8(3)	131.63(11)
O(1)–Cu(1)–O(2)	175.8(3)	176.86(10)
O(1)–Cu(1)–O(5)	86.5(3)	87.45(10)
O(1)–Cu(1)–N(1)	93.3(3)	93.67(11)
O(2)–Cu(1)–O(5)	96.6(3)	94.37(10)
O(2)–Cu(1)–N(1)	83.9(3)	84.36(15)
O(5)–Cu(1)–N(1)	174.8(4)	176.22(11)
O(2)–Cu(2)–O(3)	177.3(3)	176.68(10)
O(2)–Cu(2)–O(4)	95.9(3)	95.64(9)
O(2)–Cu(2)–N(2)	83.8(3)	85.15(10)
O(3)–Cu(2)–O(4)	86.5(3)	85.36(10)
O(3)–Cu(2)–N(2)	94.0(4)	94.22(10)
O(4)–Cu(2)–N(2)	175.8(4)	173.57(12)

Table 3 Selected bond lengths (Å) and angles (°) for **2** · $2H_2O$

Molecule A		Molecule B	
Cu(1)···Cu(2)	3.500(2)	Cu(3)···Cu(4)	3.503(1)
Cu(1)–O(1)	1.893(5)	Cu(3)–O(7)	1.905(5)
Cu(1)–O(2)	1.903(5)	Cu(3)–O(8)	1.906(5)
Cu(1)–O(5)	1.930(6)	Cu(3)–O(11)	1.931(6)
Cu(1)–N(1)	1.911(7)	Cu(3)–N(3)	1.913(6)
Cu(2)–O(2)	1.917(5)	Cu(4)–O(8)	1.915(5)
Cu(2)–O(3)	1.904(5)	Cu(4)–O(9)	1.893(5)
Cu(2)–O(4)	1.936(6)	Cu(4)–O(10)	1.929(6)
Cu(2)–N(2)	1.914(7)	Cu(4)–N(4)	1.909(7)
Cu(1)–O(2)–Cu(2)	132.8(3)	Cu(3)–O(8)–Cu(4)	132.9(3)
O(1)–Cu(1)–O(2)	177.2(2)	O(7)–Cu(3)–O(8)	177.9(2)
O(1)–Cu(1)–O(5)	86.8(2)	O(7)–Cu(3)–O(11)	87.6(2)
O(1)–Cu(1)–N(1)	93.2(3)	O(8)–Cu(3)–O(11)	94.4(2)
O(2)–Cu(1)–N(1)	85.2(3)	O(7)–Cu(3)–N(3)	93.8(3)
O(2)–Cu(1)–O(5)	94.7(2)	O(8)–Cu(3)–N(3)	84.2(2)
O(5)–Cu(1)–N(1)	177.8(3)	O(11)–Cu(3)–N(3)	176.2(3)
O(2)–Cu(2)–O(3)	175.4(2)	O(8)–Cu(4)–O(9)	178.3(2)
O(2)–Cu(2)–O(4)	94.0(2)	O(8)–Cu(4)–O(10)	93.9(2)
O(3)–Cu(2)–O(4)	88.2(2)	O(9)–Cu(4)–O(10)	87.2(2)
O(2)–Cu(2)–N(2)	84.7(3)	O(8)–Cu(4)–N(4)	84.0(3)
O(3)–Cu(2)–N(2)	93.6(3)	O(9)–Cu(4)–N(4)	94.9(3)
O(4)–Cu(2)–N(2)	174.1(3)	O(10)–Cu(4)–N(4)	175.9(3)

The cyclic structure resembles cyclohexane in its chair configuration. Since there are only four water molecules instead of six, this aggregate structure can be best described as pseudo-hexameric. The cyclic structure of $(H_2O)_6$ in a chair conformation is a rare occurrence. It has been previously reported in liquid helium droplets or in organic supramolecular networks.[35] Studies on such water assemblies have shown that a cyclic structure is energetically less favorable in comparison to prism, cage, book and boat conformations.[4] The average O···O···O angle of ~116.5° in the cyclic structure shows a minor deviation from the C–C–C bond angle of 111.05° in the chair conformation of cyclohexane. This angle is, however, in very good agreement with the 116.5° observed[36] in liquid water hexamer, but deviates considerably from the angle of 109.3° in hexagonal ice.[37] The pseudo-hexameric moiety does have an inversion center and three C_2 axes bisecting the three pairs of oxygen atoms O(13)#1, O(13)#2; O(14), O(14)#3; O(6), O(6)#3 as in cyclohexane, but, unlike cyclohexane, it does not possess a C_3 or S_6 axis. Among the structurally characterized cyclic hexamers, the one reported by Custelcean and co-workers has an ice-like chair conformation of six water molecules trapped in an organic host lattice derived from 2,4-dimethyl-5-amino-benzo-[*b*]-1,8-naphthyridine.[10] A planar high energy cyclic

Table 4 Selected hydrogen-bonding parameters in the supramolecular structures of $\mathbf{1}\cdot 2H_2O$, $\mathbf{2}\cdot 2H_2O$ and $\mathbf{3}\cdot 0.5H_2O$

	O–H···O	d(O···O)/Å	d(H···O)/Å	∠O–H···O/°	O···O···O	∠O···O···O/°
$\mathbf{1}\cdot 2H_2O^a$	O(8)–H···O(7)	2.92(3)	2.01	159.7	O(3)#3···O(7)···O(8)	95.3
	O(7)–H···O(8)#2	2.98(3)	2.23	135.5	O(3)#3···O(7)···O(8)#2	98.9
	O(6)#3–H···O(1)^d	2.67(1)	1.84	140.5	O(7)···O(8)···O(7)#1	114.3
	O(7)–H···O(3)#3	2.78(2)	1.86	163.0	O(8)···O(7)···O(8)#2	116.0
$\mathbf{2}\cdot 2H_2O^b$	O(14)–H···O(13)#2	2.73(1)	2.00	131.5	O(6)···O(13)#1···O(14)#3	111.7
	O(13)#1–H···O(1)#1	2.85(1)	1.93	160.1	O(13)#1···O(6)···O(14)	130.8
	O(13)#1–H···O(6)	2.78(1)	1.86	161.4	O(6)···O(14)···O(13)#2	107.1
	O(14)–H···O(9)#3	2.87(1)	2.28	117.9	—	—
	O(6)–H···O(14)	2.77(1)	2.04	130.3	—	—
	O(12)–H···O(16)#2	2.63(1)	1.68	159.3	—	—
	O(15)#2···O(16)#2	2.72(2)	—	—	—	—
	O(15)#2···O(7)#2	2.84(1)	—	—	—	—
	O(16)#2···O(3)#2	2.74(1)	—	—	—	—
$\mathbf{3}\cdot 0.5H_2O^c$	O(7)#2···O(1)	2.94(1)	—	—	—	—
	O(7)#3···O(1)	2.92(1)	—	—	—	—
	O(6)–H···O(3)#1^e	2.81(1)	2.06	164.6	—	—

[a] Symmetry codes: #1: $x - 1/2, -y, -z+1$; #2: $x+1/2, -y, -z+1$; #3: $x+1/2, -y+1, -z+1$. [b] Symmetry codes: #1: $-x+2, -y+1, -z+1$; #2: $x+1, y, z$; #3: $-x+3, -y, -z$. [c] Symmetry codes: #1: $x+1, +y, +z$; #2 $-x, +y-1/2, -z+1/2+1$; #3 $x, -y+1/2+1, +z+1/2$. [d] O(6)#3–H, 0.98 Å. [e] O(6)–H, 0.78 Å.

form of water aggregates trapped in an organic supramolecular host based on bismesityl-3,3′-dicarboxylic acid has been reported by Venugopalan and co-workers.[11] Gibson and co-workers have reported a supramolecular cryptand structure presenting a pseudo-hexameric cyclic chair form of water molecules.[12] Cyclic hexameric water aggregates in chair conformation are also known to form in 3D metal-organic framework structures of Ce(III) and Pr(III) with pyridine-2,6-dicarboxylic acid.[15]

The quasi-linear arrangement of water molecules in $\mathbf{2}\cdot 2H_2O$ involves two positionally disordered water molecules [O(15) and O(16) as major (site occupancy 0.7) and O(15A), O(16A) as minor (site occupancy 0.3) components], along with the pendant *p*-hydroxy group of the carboxylate (Fig. 5). A distance of 2.72(2) Å between O(15)#2 and O(16)#2 belonging to two water molecules suggests moderately strong hydrogen-bonding interactions. The terminal O(16) water is relatively strongly hydrogen-bonded to the host structure, involving the pendant *p*-hydroxy group of the carboxylate and the phenoxo atom O(3) and giving O···O distances of ~2.6 and ~2.7 Å, respectively. The central water molecule is relatively unsupported, showing a weakly hydrogen-bonding interaction with the phenoxo oxygen atom [O(7)#2···O(15)#2, 2.84(1) Å]. The relatively short distance of 2.32(3) Å between O(15A)#2 and O(15A)#4 could be related to the positional disorder of the central two water molecules among four sites.

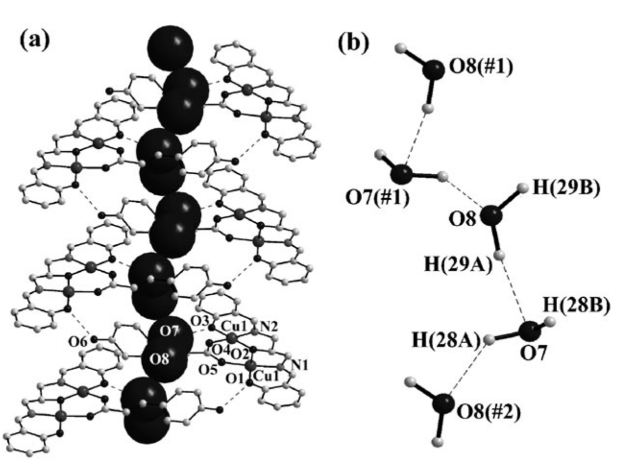

Fig. 2 (a) Perspective view of the self-assembled helical supramolecular host structure of $[Cu_2L(O_2C\text{–}CH{=}CH\text{–}C_6H_4\text{-}p\text{-}OH)]\cdot 2H_2O$ ($\mathbf{1}\cdot 2H_2O$), showing "free" and "host-bound" water molecules in the water chain. (b) Hydrogen-bonding network in the helical water chain.

Complex **3**, as a hemi-hydrate, crystallizes in the monoclinic space group $P2_1/c$. The structural features of the dicopper(II) core are similar to the other two complexes, having a $\{Cu_2(\mu\text{-}OR)(\mu\text{-}O_2CR)\}$ core. The Cu···Cu distance is 3.464(2) Å. The $\{Cu_2L\}^+$ unit has a planar structure. The carboxylate has a $\text{–}CH_2CH_2\text{–}$ spacer with two sp^3-hybridized carbon atoms; such a conformation leads to the formation of a one-dimensional chain-like supramolecular structure due to hydrogen-bonding interactions involving the pendant *p*-hydroxy group of the carboxylate and one phenoxo oxygen atom of the Schiff base [Fig. 6(a)]. The *p*-hydroxy group in $\mathbf{3}\cdot 0.5H_2O$ makes an angle of ~65° with the $Cu_2N_2O_5$ plane. The angle between the $\text{–}CH_2CH_2\text{–}$ spacer and the aromatic ring of the carboxylate is ~129°. The positionally disordered lattice water molecule acts as a linker between two supramolecular 1D chains [Fig. 6(b)].

Thermal and powder XRD studies

The thermal stability of the water molecules in complexes $\mathbf{1}\cdot 2H_2O$ and $\mathbf{2}\cdot 2H_2O$ has been studied by thermogravimetric

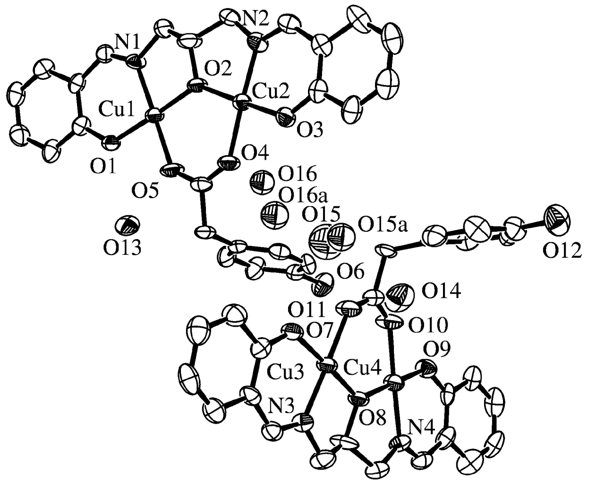

Fig. 3 ORTEP views of the two molecules of $[Cu_2L(O_2C\text{–}CH_2\text{–}C_6H_4\text{-}p\text{-}OH)]\cdot 2H_2O$ ($\mathbf{2}\cdot 2H_2O$) in the crystallographic asymmetric unit, showing 50% probability thermal ellipsoids and the atom numbering scheme for the metal and the heteroatoms. Atoms O(15), O(16) and O(15A), O(16A) are positionally disordered, having site occupancies of 0.7 and 0.3, respectively.

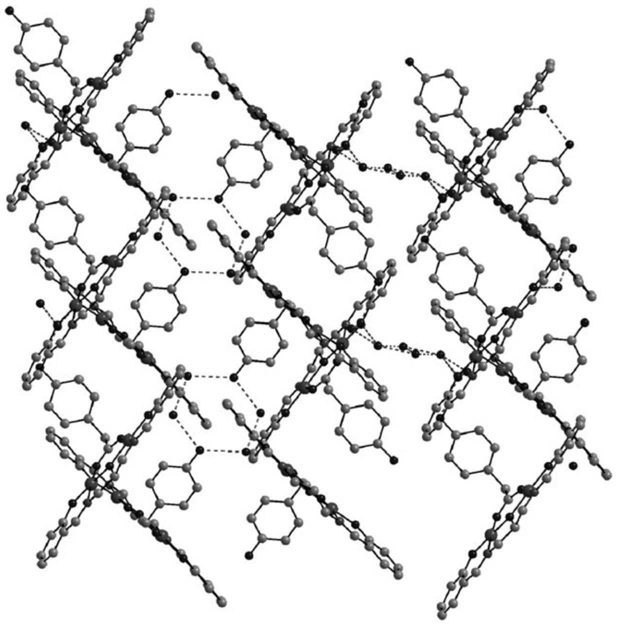

Fig. 4 A perspective view of the self-assembled supramolecular structure in [$Cu_2L(O_2C–CH_2–C_6H_4$-*p*-OH)]·$2H_2O$ (**2**·$2H_2O$).

analysis (TGA) and differential scanning calorimetry (DSC). The reversibility of the dehydration process was probed by powder X-ray diffraction studies. The TGA of **1**·$2H_2O$ gives a weight loss of ~4.5% in the temperature range 25–140 °C due to loss of two water molecules (Fig. 7). The lability of the water molecules is evidenced from significant loss of water even at 25 °C. The experimental TGA data show a sharp weight loss from the beginning of the experiment, hence rendering the observed water loss percentage (4.6%) less than the theoretical value of 5.8%. The DSC experiments reveal two endotherms at 61.5 and 88.5 °C, corresponding to the loss of "free" and "host-bound" water molecules, respectively, with the process of water loss beginning below 25 °C (Fig. 8). The overall change of enthalpy per water molecule is ~36 kJ mol^{-1}. The TGA of **2**·$2H_2O$ shows a weight loss of 5.85% (calculated weight loss 5.9%) within 100–150 °C, corresponding to the loss of both water molecules (Fig. 7). The DSC plot of **2**·$2H_2O$ displays one endotherm at 131 °C with a shoulder at ~126 °C, due to successive loss of both water molecules (Fig. 8). The overall change in enthalpy per water molecule is ~26 kJ mol^{-1}.

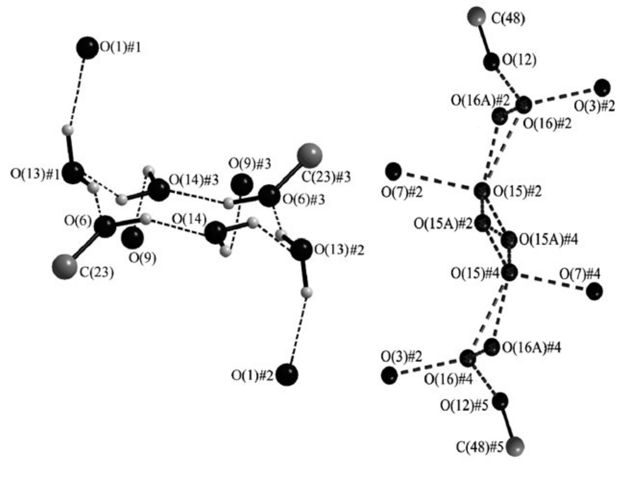

Fig. 5 The hydrogen-bonding networks in the cyclic pseudo-hexameric and the quasi-linear water aggregates in [$Cu_2L(O_2C–CH_2–C_6H_4$-*p*-OH)]·$2H_2O$ (**2**·$2H_2O$).

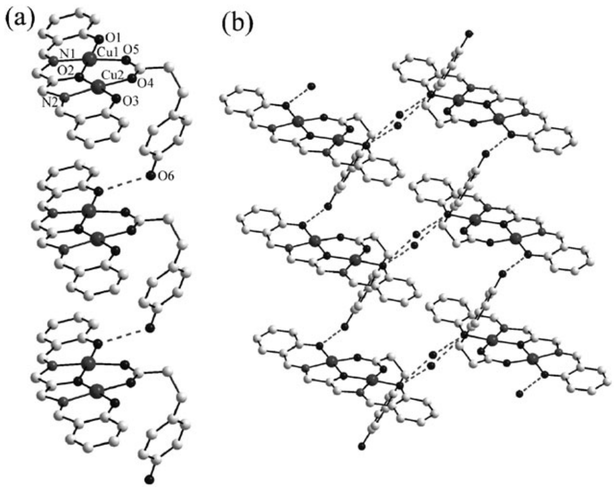

Fig. 6 (a) Perspective view of the 1D chain supramolecular host structure in [$Cu_2L(O_2C–CH_2CH_2–C_6H_4$-*p*-OH)]·$0.5H_2O$, (**3**·$0.5H_2O$), showing atom labelling for the metal and the heteroatoms. (b) Hydrogen-bond linkage of two chains by lattice water.

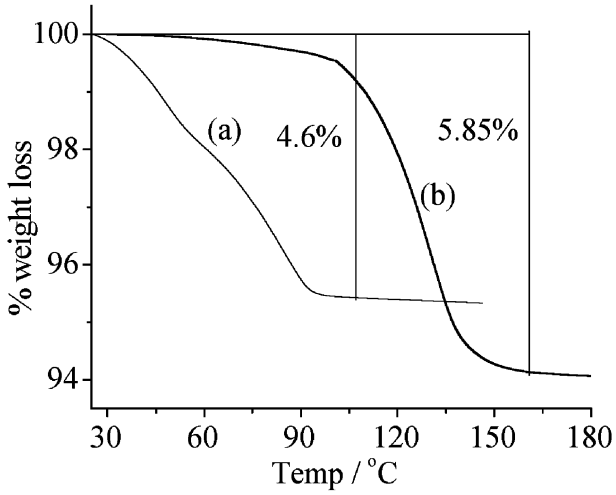

Fig. 7 Thermogravimetric plots of (a) **1**·$2H_2O$ and (b) **2**·$2H_2O$, showing weight loss of the sample with increasing temperature.

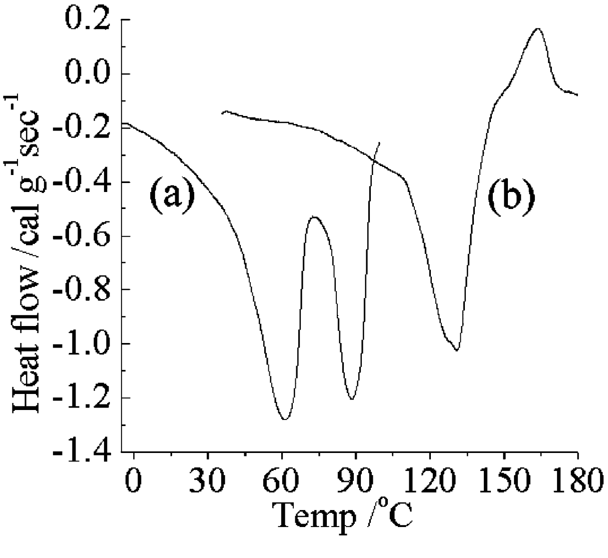

Fig. 8 Differential scanning calorimetric plots of the complexes (a) **1**·$2H_2O$ and (b) **2**·$2H_2O$, showing endotherms due to loss of water molecules.

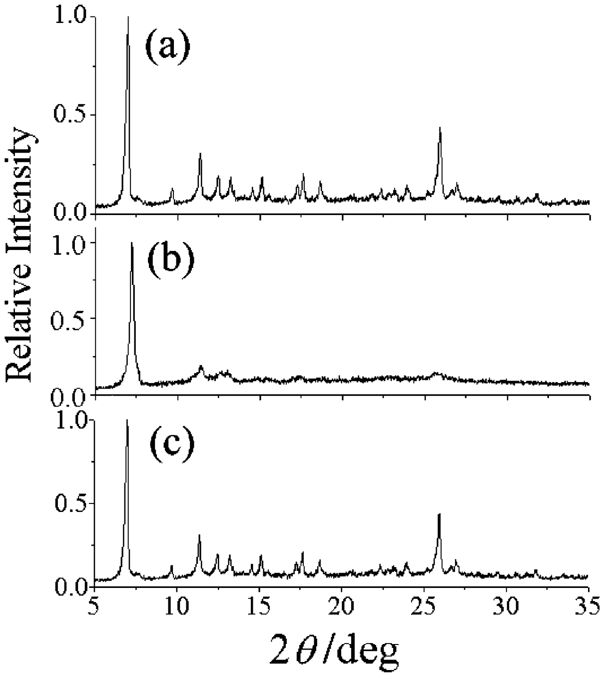

Fig. 9 Powder XRD plots for (a) $1 \cdot 2H_2O$, (b) on dehydrating the sample and (c) after rehydration.

The water aggregates in $2 \cdot 2H_2O$ have a significantly higher thermal stability than those in $1 \cdot 2H_2O$.

The reversibility of the processes involving water loss and subsequent addition of lattice water molecules, along with their effect on the supramolecular structure, have been studied by the powder XRD method. Complex $1 \cdot 2H_2O$, upon dehydration at 60 °C under vacuum, shows XRD features that closely resemble the original sample with minor variations but significant broadening of the pattern (Fig. 9). The sample on subsequent rehydration gives an XRD pattern that is similar to that of the original sample. The results indicate reversible loss and formation of the helical water chain in the pore of the self-assembled supramolecular structure of the *p*-hydroxycinnamate dicopper(II) Schiff base complex. The powder XRD data for $2 \cdot 2H_2O$, however, reveal significant structural changes upon loss of the lattice water molecules (Fig. 10). The sample on subsequent rehydration recovers the original XRD pattern with some variations. Structural change upon loss of water is expected for this complex as the water molecules are an integral part of the supramolecular structure (Fig. 4). The powder XRD patterns of $3 \cdot 0.5H_2O$ upon dehydration and subsequent rehydration are similar to the original pattern, suggesting reversibility of the water loss and gain processes (Fig. 11).

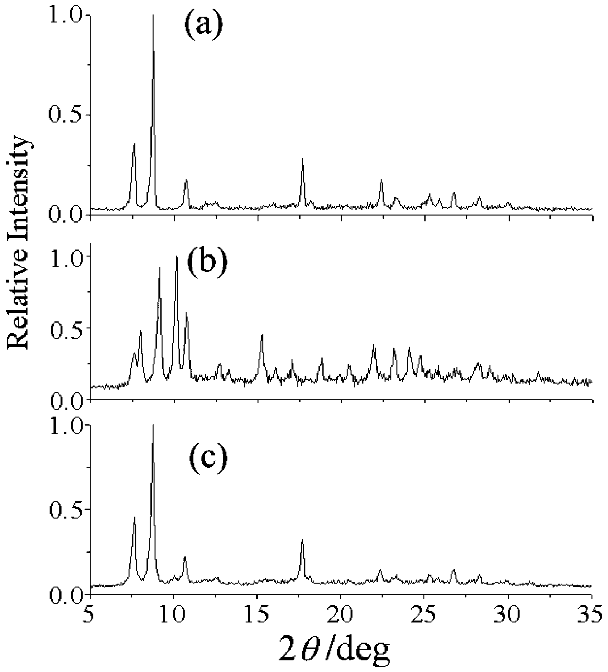

Fig. 10 Powder XRD plots for (a) $2 \cdot 2H_2O$, (b) on loss of water and (c) on subsequent rehydration.

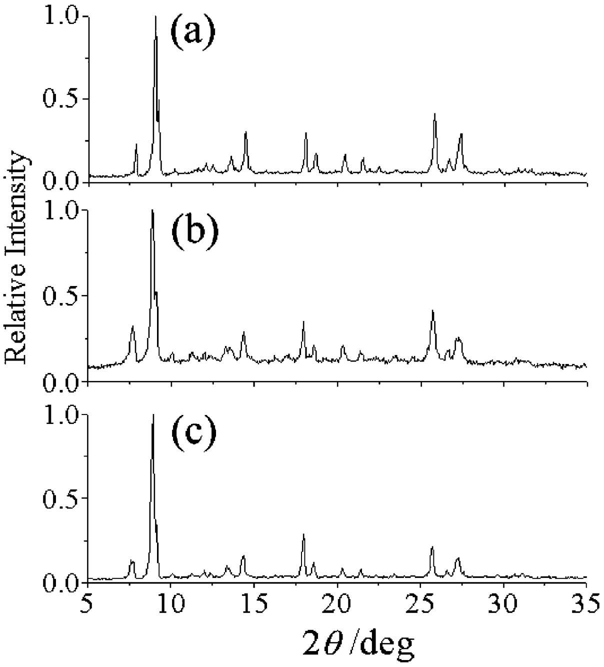

Fig. 11 Powder XRD data for (a) $3 \cdot 0.5H_2O$, (b) on removal of lattice water and (c) on subsequent rehydration.

Conclusion

We have synthesized three new asymmetrically double-bridged dicopper(II) complexes $[Cu_2L(O_2C–X–C_6H_4\text{-}p\text{-}OH)]$ (**1–3**) containing pentadentate trianionic Schiff base (L) and carboxylate ligands. The carboxylate ligands, having different spacers, $–CH{=}CH–$, $–CH_2–$ and $–CH_2CH_2–$, show noticeable stereocontrol effects on the formation of a variety of self-assembled supramolecular structures, involving the pendant hydroxy groups of the carboxylates and the phenoxo oxygen atoms of the Schiff bases.

The complexes crystallize with lattice water molecules that arrange in the form of linear chains or cyclic structures during the self-assembly processes. Complex $1 \cdot 2H_2O$, with the *p*-hydroxycinnamate ligand, forms a helical supramolecular host structure that stabilizes a helical chain of water molecules, with reversible loss and gain of the water chain during dehydration and subsequent hydration processes. Complex $1 \cdot 2H_2O$ exemplifies a potential model for the single file water arrangements in helical membrane proteins with aqua pores for transmembrane water permeation or proton transport. Complex $2 \cdot 2H_2O$ presents a supramolecular structure that stabilizes a rare pseudo-hexameric cyclic chair conformation of the water aggregate and a quasi-linear arrangement of water molecules. The water loss from the structure and subsequent hydration take place essentially in a reversible fashion although the dehydrated sample displays significant change of the host structure for $2 \cdot 2H_2O$. The $–CH_2CH_2–$ spacer of the carboxylate gives a new 1D chain supramolecular structure in $3 \cdot 0.5H_2O$ and the lattice water molecule acts as a linker of two such chains.

This work demonstrates the stereocontrol effect of the carboxylate spacers in the formation of a variety of supramolecular structures that stabilize water aggregates of novel conformations.

Acknowledgements

The authors are thankful to the Department of Science and Technology, Government of India, for financial support (Grant SP/S1/F-01/2000) and for the CCD diffractometer facility. Thanks are due to Prof. S. Ramakrishnan of our department for the thermal analysis data, Prof. T. N. Guru Row of the Solid State and Structural Chemistry Unit for the powder XRD data, and the Convener of Bioinformatics Center of our Institute for database search.

References

1 (*a*) R. Ludwig, *Angew. Chem., Int. Ed.*, 2001, **40**, 1808; (*b*) M. Henry, *Chem. Phys. Chem.*, 2002, **3**, 607.

2 (*a*) K. Bhattacharyya, *Acc. Chem. Res.*, 2003, **36**, 95; (*b*) M. Matsumoto, S. Saito and I. Ohmine, *Nature (London)*, 2002, **416**, 409.

3 (*a*) L. J. Barbour, G. W. Orr and J. L. Atwood, *Nature (London)*, 1998, **393**, 671; (*b*) L. J. Barbour, G. W. Orr and J. L. Atwood, *Chem. Commun.*, 2000, 859.

4 (*a*) F. N. Keutsch and R. J. Saykally, *Proc. Natl. Acad. Sci. USA*, 2001, **98**, 10533; (*b*) K. Liu, M. G. Brown, C. Carter, R. J. Saykally, J. K. Gregory and D. C. Clary, *Nature (London)*, 1996, **381**, 501; (*c*) K. Liu, J. D. Cruzan and R. J. Saykally, *Science*, 1996, **271**, 929; (*d*) F. N. Keutsch, J. D. Cruzan and R. J. Saykally, *Chem. Rev.*, 2003, **103**, 2533.

5 J. M. Ugalde, I. Alkorta and J. Elguero, *Angew. Chem., Int. Ed.*, 2000, **39**, 717.

6 W. B. Blanton, S. W. Gordon-Wylic, G. R. Clark, K. D. Jordan, J. T. Wood, U. Geiser and T. J. Collins, *J. Am. Chem. Soc.*, 1999, **121**, 3551.

7 (*a*) V. Zabel, W. Saenger and S. A. Mason, *J. Am. Chem. Soc.*, 1986, **108**, 3664; (*b*) K. Staahl, A. Kvick and S. Ghose, *Zeolites*, 1989, **9**, 303; (*c*) D. Cheng, M. A. Khan and R. P. Houser, *Inorg. Chem.*, 2001, **40**, 6858; (*d*) E. Freire, S. Baggio, J. Carlos and M. R. Baggio, *Acta Crystallogr., Sect. C*, 2002, **58**, m455.

8 L. E. Cheruzel, M. S. Pometun, M. R. Cecil, M. S. Mashuta, R. J. Wittebort and R. M. Buchanan, *Angew. Chem., Int. Ed.*, 2003, **42**, 5452.

9 S. N. Pal, N. B. Sankaran and A. Samanta, *Angew. Chem., Int. Ed.*, 2003, **42**, 1741.

10 R. Custelcean, C. Afloroaei, M. Vlassa and M. Polverejan, *Angew. Chem., Int. Ed.*, 2000, **39**, 3094.

11 J. N. Moorthy, R. Natarajan and P. Venugopalan, *Angew. Chem., Int. Ed.*, 2002, **41**, 3417.

12 F. Huang, L. N. Zakharov, A. L. Rheingold, J. W. Jones and H. W. Gibson, *Chem. Commun.*, 2003, 2122.

13 S. Supriya and S. K. Das, *New J. Chem.*, 2003, **27**, 1568.

14 C. Foces-Foces, F. H. Cano, M. Martinez-Ripoll, R. Faure, C. Roussel, R. M. Claramunt, C. Lopez, D. Sanz and J. Elguero, *Tetrahedron: Asymmetry*, 1990, **1**, 65.

15 S. K. Ghosh and P. K. Bharadwaj, *Inorg. Chem.*, 2003, **42**, 8250.

16 K. M. Park, R. Kuroda and T. Iwamoto, *Angew. Chem., Int. Ed. Engl.*, 1993, **32**, 884.

17 (*a*) R. J. Doedens, E. Yohannes and I. M. Khan, *Chem. Commun.*, 2002, 62; (*b*) A. Iida and T. Ozeki, *Acta Crystallogr., Sect. C*, 2003, **59**, i41; (*c*) A. Michaelides, S. Skoulika, E. G. Bakalbassis and J. Mrozinski, *Cryst. Growth Des.*, 2003, **3**, 487.

18 A.-Q. Wu, L.-Z. Cai, W.-T. Chen, G.-C. Guoa and J.-S. Huang, *Acta Crystallogr., Sect. C*, 2003, **59**, m491.

19 D. Konozo, M. Yasui, L. S. King and P. Agre, *J. Clin. Invest.*, 2002, **109**, 1395.

20 K. Mitsuoka, K. Murata, T. Walz, T. Hirai, P. Agre, J. B. Heymann, A. Engel and Y. Fujiyoshi, *J. Struct. Biol.*, 1999, **128**, 34.

21 R. Pomès and B. Roux, *Biophys. J.*, 1996, **71**, 19.

22 T. W. Allen, O. S. Andersen and B. Roux, *Proc. Natl. Acad. Sci. USA*, 2004, **101**, 117.

23 (*a*) F. H. Herbstein, in *Comprehensive Supramolecular Chemistry*, eds. J. L. Atwood, J. E. D. Davies, D. D. MacNicol and F. Vögtle, Pergamon, Oxford, England, 1996, vol **6**, p. 61; (*b*) J.-M. Lehn, *Supramolecular Chemistry – Concepts and Properties*, VCH, Weinheim, Germany, 1995; (*c*) M. I. Newby and N. L. Greenbaum, *Proc. Natl. Acad. Sci. USA*, 2002, **99**, 12697; (*d*) W. S. Bryant, J. W. Jones, P. E. Mason, I. A. Guzei, A. L. Rheingold, D. S. Nagvekar and H. W. Gibson, *Org. Lett.*, 1999, **1**, 1001.

24 A. Mukherjee, M. K. Saha, M. Nethaji and A. R. Chakravarty, *Chem. Commun.*, 2004, 716.

25 Y. Nishida and S. Kida, *J. Chem. Soc., Dalton Trans.*, 1986, 2633.

26 B. Bleaney and K. D. Bowers, *Proc. R. Soc. London, A*, 1952, **214**, 451.

27 O. Kahn, *Molecular Magnetism*, VCH, Weinheim, 1993.

28 A. C. T. North, D. C. Phillips and F. S. Mathews, *Acta Crystallogr., Sect. A*, 1968, **24**, 351.

29 N. Walker and D. Stuart, *Acta Crystallogr., Sect. A*, 1983, **39**, 158.

30 G. M. Sheldrick, *SHELX-97, Programs for crystal structure solution and refinement*, University of Göttingen, Göttingen, Germany, 1997.

31 C. K. Johnson, *ORTEP* (Report ORNL-5138) Oak Ridge National Laboratory, Oak Ridge, TN, 1976.

32 A. Mukherjee, M. K. Saha, I. Rudra, S. Ramasesha, M. Nethaji and A. R. Chakravarty, *Inorg. Chim. Acta*, 2004, **357**, 1077.

33 W. Mazurek, B. J. Kennedy, K. S. Murray, M. J. O'Connor, J. R. Rodgers, M. R. Snow, A. G. Wedd and P. R. Zwack, *Inorg. Chem.*, 1985, **24**, 3258.

34 R. Hoffmann, *Acc. Chem. Res.*, 1971, **4**, 1.

35 K. Nauta and R. E. Miller, *Science*, 2000, **287**, 293.

36 A. H. Narten, W. E. Thiessen and L. Blum, *Science*, 1982, **217**, 1033.

37 D. Eisenberg and W. Kauzmann, *The Structure and Properties of Water*, Oxford University Press, Oxford, 1969.